Applied Catalysis B: Environmental 117–118 (2012) 29–35

Contents lists available at SciVerse ScienceDirect

Applied Catalysis B: Environmental

journal homepage: www.elsevier.com/locate/apcatb

Modified niobia as a bifunctional catalyst for simultaneous dehydration and oxidation of glycerol

Luiz C.A. Oliveira[a,*], Marcio F. Portilho[b], Adilson C. Silva[a], Hosane A. Taroco[a], Patterson P. Souza[c]

[a] Departamento de Química, Universidade Federal de Minas Gerais, Av. Antônio Carlos 6627, Campus Pampulha, 31270-901, BH-MG, Brazil
[b] CENPES-Petrobras, Cidade Universitária, Q7. Ilha do Fundão, 21949-900, Rio de Janeiro-RJ, Brazil
[c] Centro Federal de Educação Tecnológica de Minas Gerais, CEFET-MG, Av. Amazonas 5253, 30421-169, BH-MG, Brazil

ARTICLE INFO

Article history:
Received 10 August 2011
Received in revised form
22 November 2011
Accepted 28 December 2011
Available online 6 January 2012

Keywords:
Niobia
Glycerol
Dehydration
Oxidation

ABSTRACT

The niobia (Nb_2O_5) obtained in this study was modified by pretreatment with hydrogen peroxide to produce a bifunctional catalyst ($Nb_2O_5//H_2O_2$) with both acidic and oxidizing properties. The oxidizing properties of niobia were obtained by the generation of peroxo groups on the catalyst surface. The catalytic conversion of glycerin showed high activity using H_2O_2 as the oxidant. The catalytic tests monitored by mass spectrometry (ESI-MS) suggested the formation of ethers obtained by the condensation of glycerol (m/z = 167, 223, 240). Furthermore, it was observed that the modification of the catalyst directs the formation of larger molecules such as triglycerol compared to niobia without pretreatment with H_2O_2.

1. Introduction

Compared to diesel fuel derived from petroleum, biodiesel can reduce approximately 78% of carbon dioxide emissions, considering the absorption of this small molecule by plants [1,2]. It also reduces smoke emissions by 90% and virtually eliminates emissions of sulfur oxides and can be used in any diesel engine cycle, with little or no adaptation [1–4]. In this context, biodiesel appears as a promising energy source that would cause less environmental impact, especially in reducing emissions of gases like CO_2, carbon monoxide, sulfur oxides (SOx), total hydrocarbons and most toxic hydrocarbons, which present risks to public health because of their potential carcinogenic properties [3]. Biodiesel production from various sources has been stimulated in many countries, especially in Europe. In 2008, the Brazilian government promoted a national program for the production and use of biodiesel, which provides a mixture of 2% biodiesel in diesel fuels (B2) as of 2008, and up to 10% (B5) by 2013 [3]. On the other hand, the production of this fuel has some limitations, such as the generation of large amounts of glycerol as a byproduct. Currently, the Brazilian market consumes about 40,000 tons/year of glycerol, while production has risen to about 150,000 tons/year [1]. This scenario seems to indicate that the viability of the biodiesel program is directly related to the production of new economically viable products from biodiesel byproducts, especially glycerol.

Although the use of biodiesel has many environmental benefits, the production of biodiesel results in a significant waste product, glycerol. The goal of this study is to obtain products such as di and triglycerols from glycerol using catalysts based on modified niobia. The motivation is to provide value-added products from biodiesel by-products, such as di- and tri- glycerols, which can be used as fuel additives [1].

The scientific literature presents several studies aimed at producing new compounds from glycerol [5–8]. Some researchers have studied the production of fuel additives [9], but the extreme conditions used and the difficult separation of homogeneous catalysts from the reaction medium make the process expensive. Studies of glycerol conversion have also implemented the use of heterogeneous catalysts, mainly using materials with acidic functionality such as zeolites, alumina silicates and niobium oxide [10]. Additional research has pursued the conversion of glycerol to polyglycerols and polyglycerol-esters that can be used as new materials for surfactants, lubricants, cosmetics, and food additives [6].

In recent years, niobium-based systems have received special attention due to their catalytic activity in several important chemical processes, particularly when high acidity and water tolerance are needed in the processes [11–13]. Nb_2O_5 has been widely used as a catalyst in reactions for dehydration, hydration, etherification, hydrolysis, condensation, dehydrogenation, alkylation,

* Corresponding author. Tel.: +55 31 3409 6384; fax: +55 31 34095700.
E-mail address: luizoliveira@qui.ufmg.br (L.C.A. Oliveira).

0926-3373/$ – see front matter © 2012 Elsevier B.V. All rights reserved.
doi:10.1016/j.apcatb.2011.12.043

photochemical and electrochemical polymerization and oxidation [14–17]. In this study, Nb_2O_5 was synthesized and modified by treatment with hydrogen peroxide aiming to generate a bifunctional catalyst ($Nb_2O_5//H_2O_2$), *i.e.*, with both acidic and oxidizing properties. The catalysts were tested in the simultaneous dehydration and oxidation of glycerol to obtain ethers because these compounds can be employed as bio-additives for other fuels.

2. Materials and methods

2.1. Synthesis and characterizations

Nb_2O_5 (niobia) was prepared by treating 14 g of $NH_4[NbO(C_2O_4)_2(H_2O)]\cdot(H_2O)_n$ with NaOH (50 mL, 1 mol L^{-1}), followed by heating at 60 °C for 72 h [18]. This material was used as a precursor for the preparation of treated niobia ($Nb_2O_5//H_2O_2$), obtained by treating pure niobia (300 mg) with hydrogen peroxide 30% (4 mL) in water (80 mL) for 30 min at room temperature. The yellow solid was then filtered, washed with distilled water and dried at 60 °C for 12 h.

The particle diameter distribution and zeta potential variation of aqueous suspensions of the powder as a function of pH was measured by electrophoretic mobility using a Zetasizer 3000 (from M/s Malvern Instruments Ltd., UK) equipment. The Nb_2O_5 and $Nb_2O_5//H_2O_2$ aqueous solutions were prepared in Milli-Q water at a concentration of 0.33 g L^{-1}. Disintegration of particles was achieved using sonication for 20 min. The pH levels were adjusted using solutions of KOH and HCl, both at a concentration of 0.25 mol L^{-1}.

Nitrogen adsorption/desorption isotherms were obtained on a Micromeritics ASAP-2000 instrument. The specific surface area was calculated using the BET model. The pore size distribution was calculated based on the density functional theory (DFT).

The transmission electron microscopy (TEM) images were taken with a JEOL transmission electron microscope (model JEM 2000EXII).

The IR spectra were acquired with a Shimadzu FTIR (model IRPrestige-21) with IRsolution software. Accessories were used for attenuated total reflection (ATR-8200AH with ZnSe prism). The spectra were obtained from an average of 20 scans with a resolution of 4 cm^{-1}. The wavelength range measured was 4000–400 cm^{-1} using an IRPrestige-21 detector and a DLATGS Beam splitter (KBr/Ge).

2.2. Catalytic tests

Glycerol conversion was performed using H_2O_2 (30%, v/v) as the oxidizing agent. The catalytic tests were performed at 200 °C, using 10 mL of glycerol (1.15 mol L^{-1}) and 10 mg of catalyst in the presence of H_2O_2 (0.10 mL) in a batch reactor for 3 h at pH 6. The products of the reaction were analyzed by GC–MS (Shimadzu) and electrospray ionization mass spectrometry (ESI-MS) (Agilent). The percent conversion of glycerol was investigated by integrating the peak of glycerol to the total ion content (TIC), obtained before and after the reaction with the catalyst. The parameters for the GC–MS analysis were as follows: injector temperature 200 °C, injection volume 1 mL, flow 1.3 mL min^{-1} and Column HP-5 (5% polimetilfenil siloxane). A heating curve was established at 3 °C min^{-1}, from 90 °C to 150 °C. The glycerol reaction progress was monitored with electrospray ESI-MS (Agilent-1100), allowing for the identification of intermediates formed during this reaction. ESI-MS/MS experiments were performed in the positive ion mode. The glycerol decomposition was monitored using ESI-MS in an attempt to identify molecular intermediates. The reaction samples were analyzed by introducing aliquots into the ESI source with a syringe pump at a flow rate of 5 mL min^{-1}. The spectral data obtained were averaged for 50 scans at 0.2 s each. Typical ESI-MS conditions were as follows: heated capillary temperature 150 °C, dry gas (N_2) at a flow rate of 5 L min^{-1}, spray voltage 4 kV, capillary voltage 25 V and tube lens offset voltage 25 V.

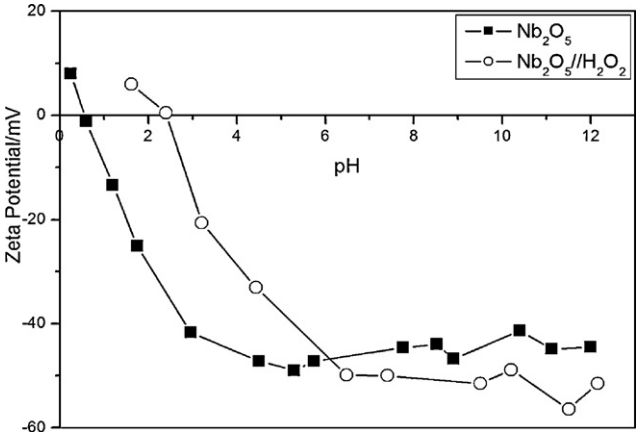

Fig. 1. The pH dependence of zeta potentials for Nb_2O_5 and $Nb_2O_5//H_2O_2$.

3. Results and discussion

3.1. Characterization of the materials

The $Nb_2O_5//H_2O_2$ produced by the method described in this paper had a yellowish (after H_2O_2 treatment) color due to the presence of peroxide groups on the surface of the niobia. These groups, which have oxidizing properties, were generated by treatment of niobia with H_2O_2. The surface changes of the materials were studied by zeta potential measurements. The variation of zeta potential with pH for the aqueous suspensions is shown in Fig. 1. The numerical value of zeta potential was found to vary with preparation conditions of the material and the medium. The zeta potential variation at pH > 6 was less than at pH < 6 in both samples. The $Nb_2O_5//H_2O_2$ suspension was more stable in alkaline medium because of its high zeta potential compared with the untreated niobia. The zeta potential was found to be approximately pH 0.57 and pH 2.40 for Nb_2O_5 and $Nb_2O_5//H_2O_2$, respectively. It is likely that there are more negative ions at the Nb_2O_5 particle surface compared to $Nb_2O_5//H_2O_2$. The treatment of Nb_2O_5 with hydrogen peroxide causes great changes in the surface of the material. The

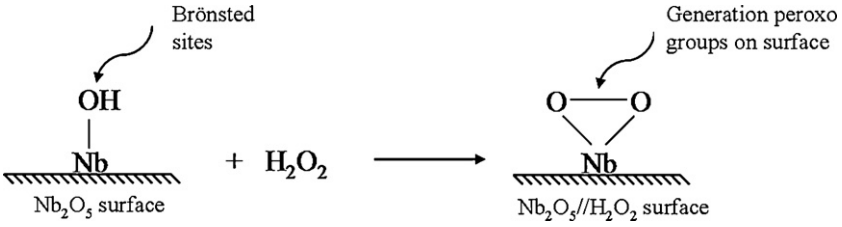

Fig. 2. Scheme of peroxo group formation on the niobia surface.

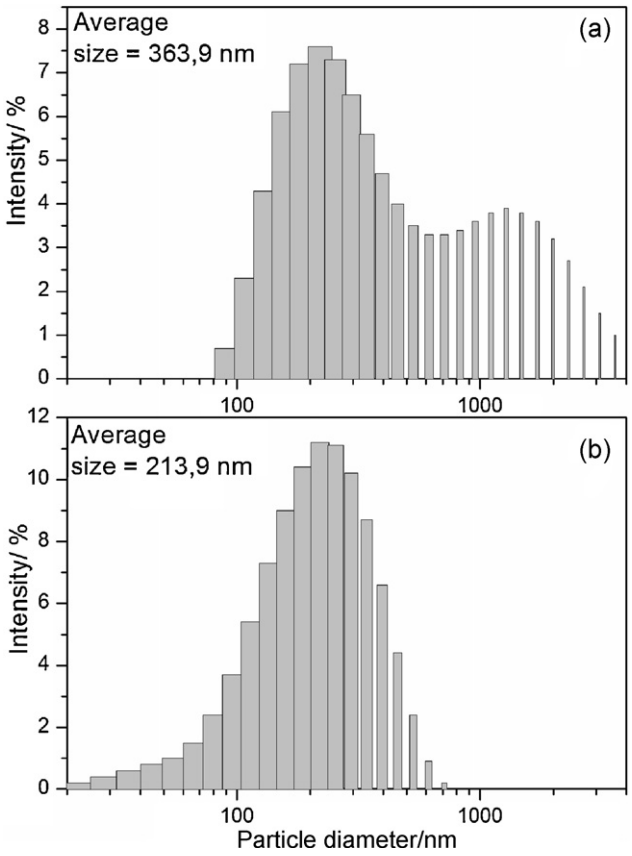

Fig. 3. Particle diameter distribution for the catalysts $Nb_2O_5//H_2O_2$ (a) and Nb_2O_5 (b).

higher pH at zero charge suggests that the H_2O_2 treatment leads to a decrease of Brönsted acid sites, forming oxidizing sites on the surface (Fig. 2). This observation was reported in previous publications from our group [11]. Based on the increase of the isoelectric point, Fig. 2 presents a simplified scheme showing peroxo group formation at the niobia surface with removal of the surface OH species, which would result in the observed change in zeta potential.

The particle diameter average for the materials was obtained and those results are presented in Fig. 3.

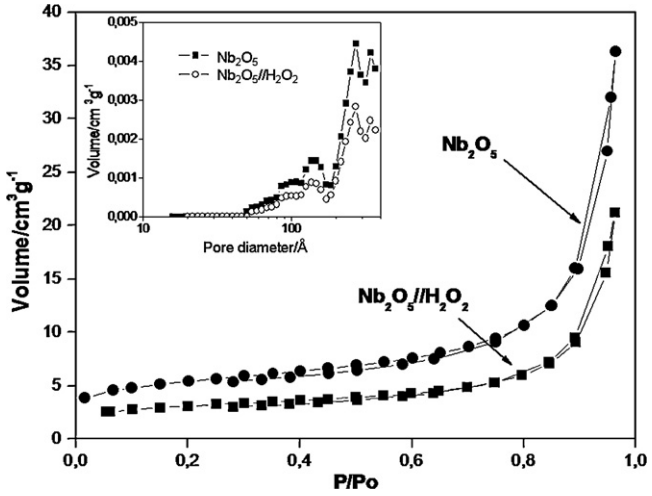

Fig. 4. N_2 adsorption/desorption isotherms at 77 K and pore distribution for Nb_2O_5 and $Nb_2O_5//H_2O_2$.

The average particle size of Nb_2O_5 and $Nb_2O_5//H_2O_2$ is 213.9 and 363.9 nm, respectively. The particle diameter distribution in Fig. 3 shows the difference in the profile of particle size after H_2O_2 treatment. These results corroborate the specific surface area data, which were observed to decrease after treatment with H_2O_2.

The textural characteristics of the niobia samples were determined by N_2 adsorption/desorption experiments. The isotherms for Nb_2O_5 and $Nb_2O_5//H_2O_2$ are shown in Fig. 4.

The specific surface areas were found to be 19 and 11 $m^2\ g^{-1}$ for Nb_2O_5 and $Nb_2O_5//H_2O_2$, respectively. The profile of the isotherms (Fig. 4) suggests a non-porous material with type III isotherms according to IUPAC classification. Interestingly, after treatment with H_2O_2 niobia shows a slight decrease of BET area, possibly due to agglomeration of particles, which is supported by observations from electron microscopy. We also observed (inset Fig. 4) that there was no significant change in the distribution of pore diameter after treatment with H_2O_2.

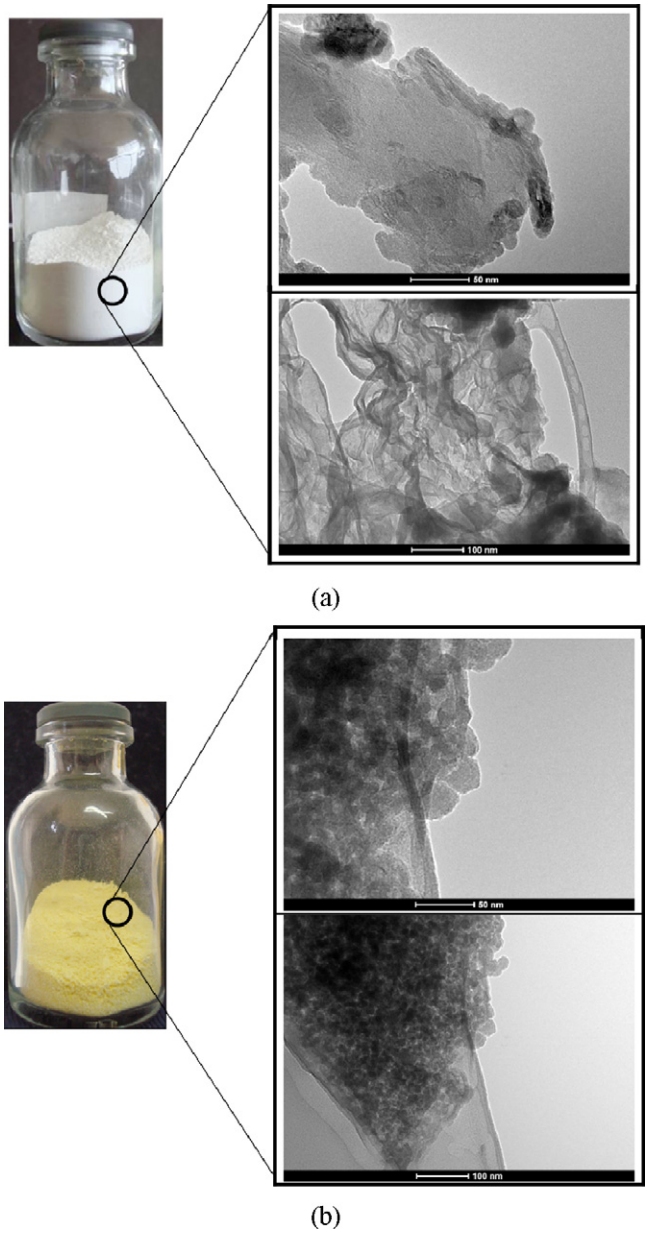

Fig. 5. TEM images of the catalysts before (a) and after (b) treatment with hydrogen peroxide.

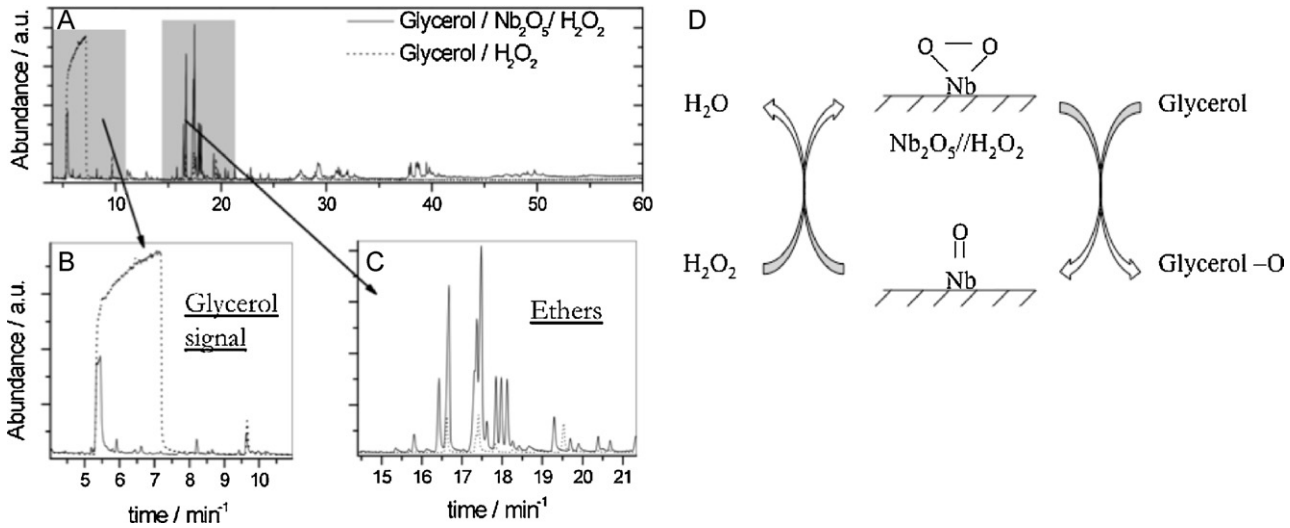

Fig. 6. Glycerol conversion profile for $Nb_2O_5//H_2O_2$ in the presence of H_2O_2 as an oxidizing agent and without catalyst (only H_2O_2) (a–c). Scheme of *in situ* regeneration of the oxidizing peroxo groups on addition of H_2O_2 (d).

The transmission electronic micrograph (TEM) studies showed that material morphology changes dramatically following treatment with hydrogen peroxide (Fig. 5a). In addition to the color, which changes from white to yellow, the images clearly showed that the Nb_2O_5 catalyst has an agglomerated sheet-like structure while the modified material ($Nb_2O_5//H_2O_2$) shows particles with irregular shape that do not order. These irregular particles may result from the non-directional arrangement of pores due to the amorphous nature of the resulting material.

3.2. Catalytic tests

3.2.1. Glycerol conversion monitored by GC–MS

Results obtained by GC–MS of the glycerol reaction showed 73% conversion after 3 h of reaction catalyzed by $Nb_2O_5//H_2O_2$. For the reaction catalyzed by Nb_2O_5, the conversion was 23%. The profile of the commercial glycerol reaction $Nb_2O_5//H_2O_2$ and H_2O_2 as an oxidizing agent is shown in Fig. 6a. In addition, the reaction containing only hydrogen peroxide (absence of catalyst) showed low activity in the reaction with glycerol, with approximately 11% conversion. The detail in Fig. 6b and c shows the difference in conversion capacity of glycerin and to further product formation in the form of ethers (di and triglycerol) by reaction with the $Nb_2O_5//H_2O_2$. In the absence of hydrogen peroxide (catalyst only) the conversion capacity was only 45.9%, showing the importance of the oxidizing agent to regenerate the peroxo groups. In fact, the reaction may involve a similar process like Mars Van Krevelen mechanism [19] that takes place in two steps: a reaction between the niobia surface and the glycerol, in which the latter is oxidized and the former reduced, followed by the reaction of the reduced oxide with added H_2O_2 to restore the initial state (Fig. 6d).

To identify the others reaction products, the reaction mixtures were monitored by ESI-MS. Furthermore, the glycerol conversion was monitored by GC–MS to quantify the catalytic activity of the catalysts.

3.2.2. Glycerol conversion monitored by ESI-MS

The spectra obtained for glycerol and the product distribution after reaction with Nb_2O_5 and $Nb_2O_5//H_2O_2$ are shown in Fig. 7.

The spectrum obtained for the glycerol standard (Fig. 7a) shows an ion with $m/z = 93$ [glycerol + H^+] with highest relative intensity. The mass spectrum of glycerol after the reaction catalyzed by Nb_2O_5 (Fig. 7b) shows a decrease in the signal $m/z = 93$ from 100% to 12%. The most intense ion with $m/z = 167$ may be associated with the protonated form of diglycerol [diglycerol + H^+]. Medeiros et al. [20] monitoring glycerol conversion by ESI-MS observed almost 90% glycerol conversion using sulfuric acid as catalyst in a homogeneous process.

The study of the fragmentation of this ion (Fig. 8a) shows two successive dehydrations [(diglycerol + H^+) – H_2O, $m/z = 149$] and

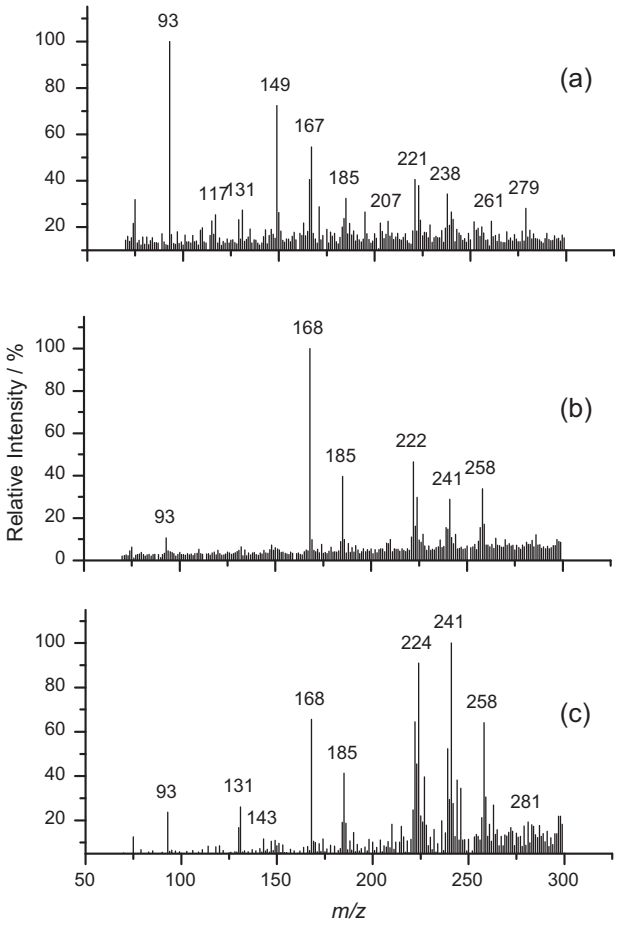

Fig. 7. ESI-(+)-MS of standard glycerol (a), after reaction with Nb_2O_5 (b) and $Nb_2O_5//H_2O_2$ (c).

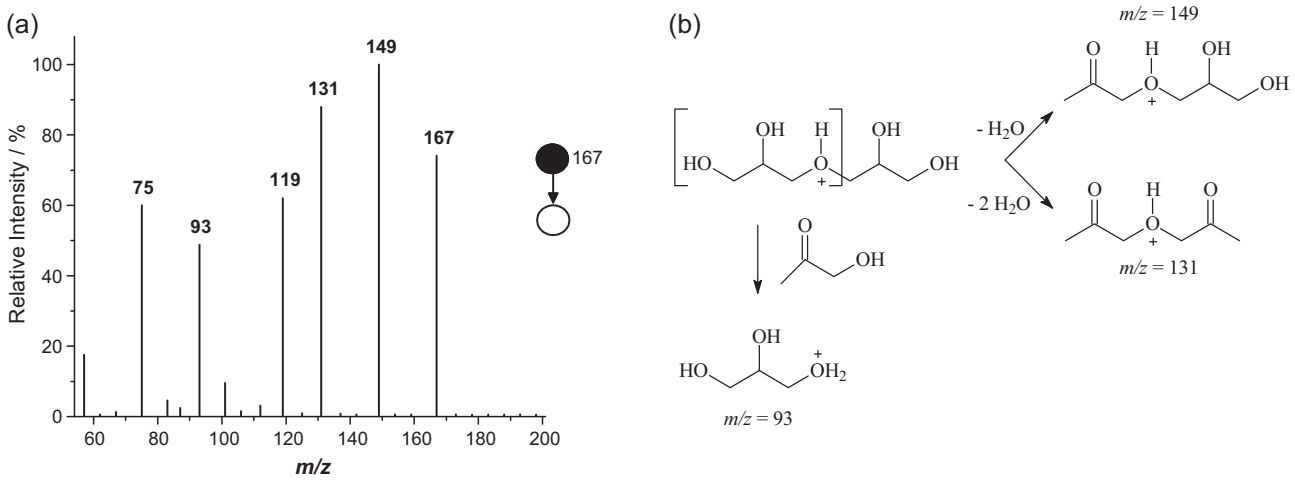

Fig. 8. ESI-(+)-MS/MS for the ion with *m/z* of 167 (25 eV) (a) and fragmentation scheme for protonated diglycerol (b).

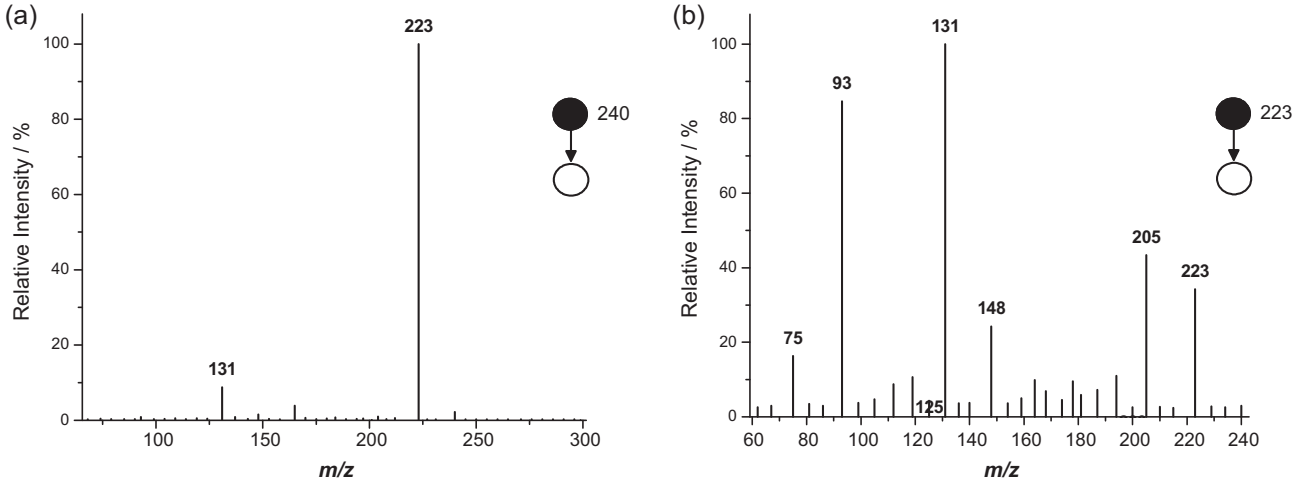

Fig. 9. ESI-(+)-MS/MS for the ions with *m/z* of 240 (15 eV) (a) and 223 (15 eV) (b).

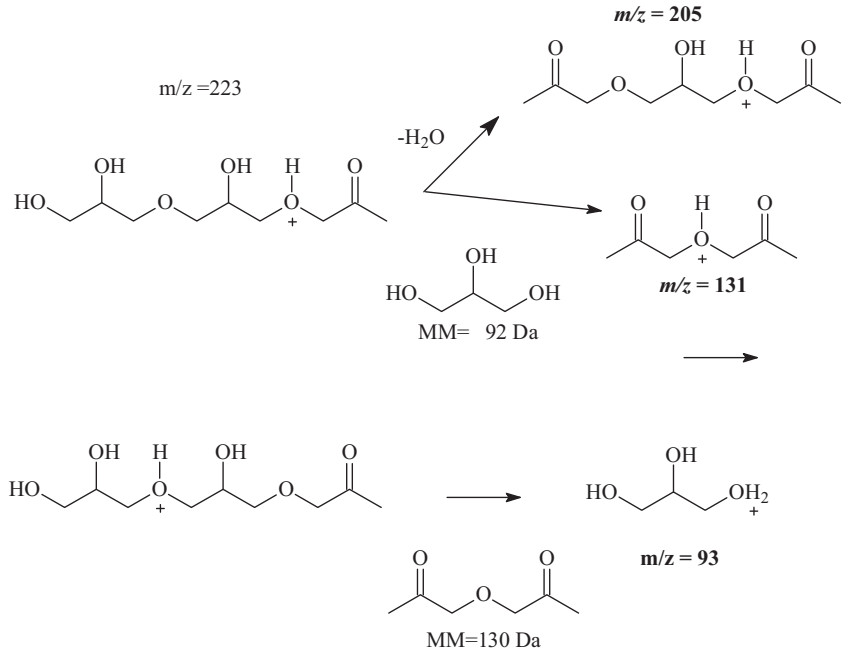

Fig. 10. Fragmentation scheme for ion with *m/z* of 223.

[(diglycerol + H^+) – $2H_2O$, m/z = 131]. Medeiros et al. [20] suggested possible structures for the fragmentation of protonated diglycerol. Some of these structures are shown in Fig. 8b.

Fig. 7c shows the mass spectrum of glycerol after reaction with $Nb_2O_5//H_2O_2$ in the presence of hydrogen peroxide. A decrease of the relative intensity of the glycerol parent ion [glycerol + H^+] m/z = 93 suggests its consumption. In this case, however, the ion with highest relative intensity has m/z = 240, followed by the ion m/z = 223. The ion with mass of 240 corresponds to protonated triglycerol and m/z = 223 correspond to the dehydrated triglycerol [(Triglycerol + H^+) – H_2O] as shown in Fig. 9a.

The increased intensity of the ion at m/z 240 and 223 compared to diglycerol indicated selectivity for this reaction towards formation of triglycerol by reaction with $Nb_2O_5//H_2O_2$. According to Trejda et al. [21], it is very difficult to obtain high selectivity of di- and tri-substituted glycerol using zeolites as catalysts. Our catalysts based on $Nb_2O_5//H_2O_2$ show good potential to fill this need. Fig. 9b shows the mass spectrum from the fragmentation (ms/ms) of ion with m/z = 223. As observed in the case of diglycerol the fragment originated from a dehydration process. In this case, however, the charge may be located at each of the two oxygen of the ether, as suggested in Fig. 10. The fragments with m/z = 131 and m/z = 93 are formed by breaking the CO bond of the ether at both positions in the protonated species.

The products of the glycerol conversion reactions were studied by infrared spectroscopy (FTIR). The FTIR normalized spectra of compounds are shown in Fig. 11.

The most intense bands seen in the spectrum of glycerol are associated with the stretching and deformation vibrations of the OH groups at 3300 and 1650 cm^{-1}, respectively. The presence of thin and well-defined bands in the region between 1200 and 1000 cm^{-1} typical of this compound and related to the stretching vibration of the CO bond can also be verified.

FTIR spectra of the products showed an increase in the intensity of the bands seen between 3000 and 2800 cm^{-1}, characteristic of methylene groups, compared to the intensities of absorption bands associated with the OH bonds of the respective spectra. The chemical structures of glycerol and its oligomers show that the ratio of the number of CH and OH groups becomes larger in the dimers and trimers. It should also be noted that bands at 994 and 921 cm^{-1} appear in the product spectra and are assigned to the out-of-plane deformation of vinyl groups.

The region between 1200 and 1000 cm^{-1} also showed change in relative intensity compared to the glycerol standard. The bands at 1110 and 1042 cm^{-1} related to the CO stretching vibrations are intensified due to the increased number of these units in the

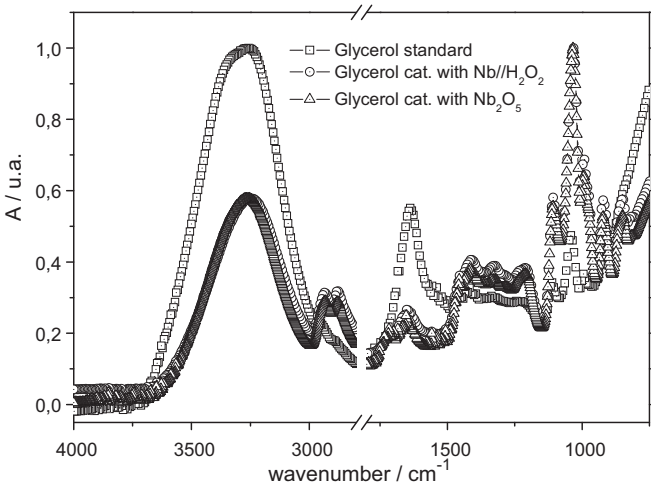

Fig. 11. Absorption spectra in the infrared region for the glycerol standard and oligomers formed after the catalysis reaction.

oligomers. Finally, the FTIR spectra of the products show a band at 1220 cm^{-1} associated with vinyl ether groups, absent in the glycerol standard. In conclusion, from the comparison of the spectra it was possible to observe variation in the relative intensity of bands, indicating a suppression of those assigned to the OH group vibrations and intensification of other groups associated with the CO and CH vibrations. This fact, coupled with the appearance of bands for vinyl ethers and vinyl groups, provided evidence of oligomer formation in the reactions catalyzed by niobia.

The catalytic activity of $Nb_2O_5//H_2O_2$ was maintained for three reaction cycles (Fig. 12a), suggesting that the surface groups can be regenerated by H_2O_2 added during the reaction. In the fourth reaction cycle the catalytic activity decrease considerably, most likely due to the formation of coke at the catalyst surface, indicated by the dark color shown in Fig. 12b. The fresh and used catalysts were analyzed by thermogravimetric analysis in air (not shown here). The Nb_2O_5 showed a mass loss related to the dehydroxylation and peroxo groups. The used $Nb_2O_5//H_2O_2$ showed a mass loss of *ca.* 12% after 300 °C likely due to the oxidation of carbon deposits formed with the glycerol reaction [1]. In order to recover the catalyst and use it again, the black solid obtained after the reaction (Fig. 12b) was treated with H_2O_2 leading to a yellow treated niobia (recovered catalyst) with peroxo groups on its surface (Fig. 12b). The recovered material presented a very similar catalytic activity compared to a fresh catalyst.

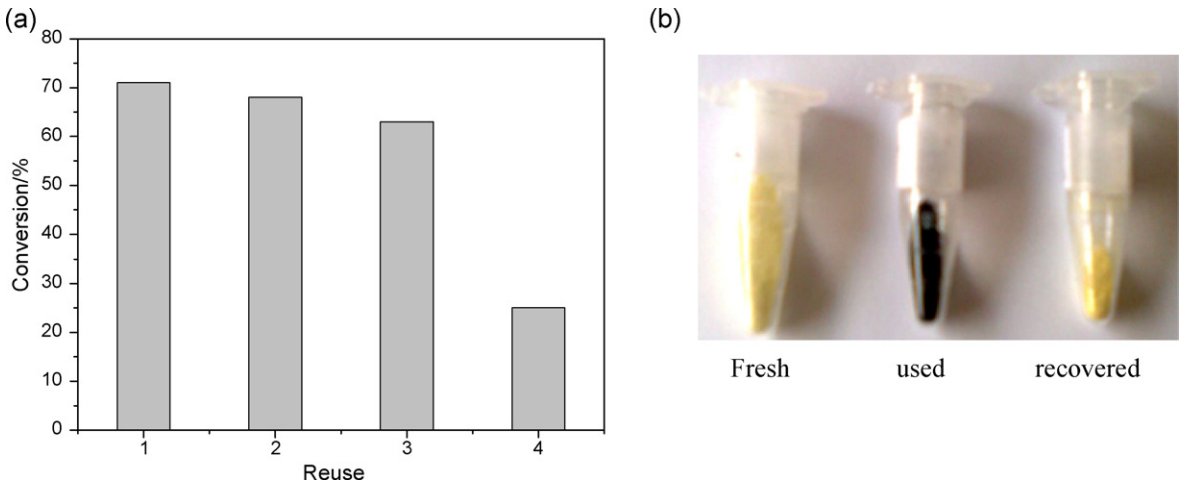

Fig. 12. Scheme for the reaction at a niobia surface (a) and for the regeneration of oxidizing groups in the presence of H_2O_2 (b).

4. Conclusion

Modified niobia catalysts presented in this study show great potential for the conversion of glycerol using H_2O_2 as an oxidant. Furthermore, products with potential industrial applications were obtained from the reactions, such as ethers generated by the reaction of glycerol with peroxo groups generated at the niobia surface. Synthetic bio-molecules were also obtained, which may be applied as additives for fuels. The niobia was synthesized and modified by the addition of hydrogen peroxide, generating a bifunctional catalyst with highly oxidizing peroxo groups at its surface. The modified catalyst could be reused, showing good activity for three reaction cycles, but the deactivation hindered its activity, most likely due to coke formation on the surface.

Acknowledgments

The authors express their thanks to the PRPq-UFMG, PETROBRAS, FAPEMIG, CNPq, CAPES and CBMM.

References

[1] C.J.A. Mota, C.X.A. Silva, V.L.C. Golncalves, Quim. Nova 32 (2009) 639–648.
[2] A.C. Pinto, L.N. Guarieiro, M.J.C. Resende, N.M. Ribeiro, E.A. Torres, W.A. Lopes, P.A.D. Pereira, J.B. Andrade, J. Braz. Chem. Soc. 16 (2005) 1313.
[3] Y.C. Lin, W.J. Lee, H.W. Li, C.B. Chen, G.C. Fang, P.J. Tsai, Atmos. Environ. 40 (2006) 1601–1609.
[4] J. Yang, J. Huang, H. Qiu, S. Rozelle, M.A. Sombilla, Appl. Energy 86 (2009) S37–S46.
[5] A. Corma, G.W. Huber, L. Sauvanaud, P. O'Connor, J. Catal. 257 (2008) 163–171.
[6] J.M. Clacens, Y. Pouilloux, J. Barrault, Appl. Catal. A-Gen. 227 (2002) 181–190.
[7] R. Garcia, M. Besson, P. Gallezot, Appl. Catal. A-Gen. 127 (1995) 165–176.
[8] Patent A. Neher et al. Process for production of acrolein. Degussa Aktiengesellschaft, US5387720, 1995.
[9] F. Frusteri, F. Arena, G. Bonura, C. Cannilla, L. Spadaro, O. Di Blasi, Appl. Catal. A-Gen. 367 (2009) 77–83.
[10] E. Lotero, Y. Liu, D.E. Lopez, K. Suwannakarn, D.A. Bruce, J.G.G. Junior, Ind. Eng. Chem. Res. 44 (2005) 5353–5363.
[11] L.C.A. Oliveira, T.C. Ramalho, E.F. Souza, M. Gonçalves, D.Q.L. Oliveira, M.C. Pereira, J.D. Fabris, Appl. Catal. B-Environ. 83 (2008) 169–176.
[12] A.C. Silva, D.Q.L. Oliveira, L.C.A. Oliveira, A.S. Anastácio, T.C. Ramalho, J.H. Lopes, H.W.P. Carvalho, C.E.R. Torres, Appl. Catal. A-Gen. 357 (2009) 79–84.
[13] I.R. Guimaraes, L.C.A. Oliveira, P.F. Queiroz, T.C. Ramalho, M.C. Pereira, J.D. Fabris, J.D. Ardisson, Appl. Catal. A-Gen. 347 (2008) 89–93.
[14] I. Nowak, M. Ziolek, Chem. Rev. 99 (1999) 3603–3624.
[15] K. Tanabe, Catal. Today 78 (2003) 65–77.
[16] M.A. Abdel-Rehim, A.C.B. Santos, V.L.L. Camorim, A.C. Faro Jr, Appl. Catal. A-Gen. 305 (2006) 211–218.
[17] A.G.S. Prado, L.B. Bolzon, C.P. Pedroso, A.O. Moura, L.L. Costa, Appl. Catal. B-Environ. 82 (2008) 219–224.
[18] A. Esteves, L.C.A. Oliveira, T.C. Ramalho, M. Gonçalves, A.S. Anastácio, H.W.P. Carvalho, Catal. Commun. 10 (2008) 330–332.
[19] J.M. Thomas, W.J. Thomas, Introduction to the Principles of Heterogeneous Catalysis, Academic Press, London, 1967.
[20] M.A. Medeiros, M.H. Araujo, R. Augusti, L.C.A. de Oliveira, R.M. Lago, J. Braz. Chem. Soc. 20 (2009) 1667–1673.
[21] M. Trejda, K. Stawicka, M. Ziolek, Appl. Catal. B: Environ. 103 (2011) 404–412.